Flow-induced transition from cylindrical to layered patterns in magnetorheological suspensions

S. Cutillas,[1] G. Bossis,[1] and A. Cebers[1,2]
[1]*Laboratoire de Physique de la Matière Condensée, CNRS UMR 6622, Parc Valrose, 06108 Nice Cedex 2, France*
[2]*Institute of Physics, Latvian Academy of Sciences, Salaspils 1, LV-2169, Latvia*
(Received 24 February 1997)

A transition from a hexagonal to a layered pattern is observed when a magnetic suspension structured by a magnetic field is submitted to an oscillating shear flow. This transition occurs at a well-defined strain $\gamma_o = 0.15$, which is found to be independent of the cell thickness, the intensity of the magnetic field, and the Péclet number. This layered pattern is stable in the absence of the flow if it has been formed at a Péclet number higher than unity. In this domain the period of the stripes increases with the intensity of the magnetic field and decreases with the initial volume fraction of magnetic particles. These features are explained by a model based on the minimization of the magnetic energy and on the equilibrium of osmotic, hydrodynamic, and magnetic pressures. [S1063-651X(98)02101-1]

PACS number(s): 82.70.Kj, 47.10.+g, 83.10.−y

I. INTRODUCTION

The competition between long-range repulsive and short-range attractive interactions determines the pattern formation for many physical systems where dipolar or Coulombic forces are present [1]. The long-range repulsive forces tend to divide the matter in order to reduce the repulsive energy, whereas attractive forces such as those giving rise to surface tension or a Lorentz field tend to gather the matter in a single unit. This observation explains that patterns formed in very different physical systems can have striking similarity. For instance, the undulation instability of a striped pattern that gives rise to the chevron structure is observed in magnetic liquids [2], thin ferromagnetic films [3], and some systems governed by reaction-diffusion equations [4]. In magnetic liquids, the change of period of a striped pattern with the amplitude of the external magnetic field has been successfully predicted when the effective surface tension at the boundary between the two phases is known [5,6]. In the limiting case where the period of the structure is much larger than the thickness of the layer, this approach can also describe the structures of other systems such as amphiphile monolayers [7].

Pattern formation has also been observed in electrorheological (ER) and magnetorheological (MR) suspensions, which are suspensions of much larger (1–10 μm) paramagnetic or dielectric particles. Well-defined structures formed with cylindrical aggregates aligned with the magnetic field and arranged in an hexagonal pattern have been observed in MR fluids at low volume fraction [8,9]. The transformation of these cylindrical structures into a striped pattern in the presence of a shear flow was observed many years ago [10], but never carefully studied. It is the purpose of this paper to report on this transition and to analyze it by adapting the models used for ferrofluids. It is worth noting that if the cylindrical structure is found at a low volume fraction, a layered structure is predicted to have a lower energy at higher volume fractions [11]. Striped patterns also have been observed in ER fluids in the presence of oscillating shear flow [12] and also predicted by numerical simulations in steady shear flows [13,14], but their origin is different due to the absence of a depolarizing field that is canceled by the charges brought by the electrodes. This important difference from the magnetic case and also the presence of an ionic polarization in ER suspensions that can be out of phase with the shear flow make the interpretation quite different. In this paper we shall limit our discussion to MR fluids only.

There are two main differences between magnetorheological suspensions and ferrofluids. First, the aggregated phase of a MR suspension is compressible and its volume fraction will be determined by a balance between the magnetic pressure and the osmotic pressure. Actually, the quite unusual observation [15] that the elongation of an agglomerate of particles in MR suspension decreases when the magnetic field increases can be explained by taking into account the change of volume fraction of particles inside the agglomerate [16]. Second, the surface tension only comes from the difference between the local magnetic field inside the aggregate and the one on the boundary [17,18]. As the magnetic moment of the micronic particles is induced by the field, all the structure in MR suspensions is determined by the competition between field-induced dipolar forces; this is not necessarily the case in ferrofluids, where the surface tension due to the interactions between the permanent dipoles is also important.

In this paper we are going to present some experimental results on the transition from a cylindrical to a striped pattern in a MR suspension (Sec. III) and on the period of this layered pattern (Sec. IV A). In particular, we shall show that, in contrast to incompressible magnetic liquids, the period of the layered structure increases with the external magnetic field strength. Also, the undulation instability of the striped structure appears when the field is decreased (instead of increased in ferrofluids [2]). In Sec. IV B and IV C these differences of behavior from a ferrofluid are explained by a model that takes into account the compression of the stripes by the magnetic field. Section V is devoted to a discussion of the model. We shall in particular emphasize how the presence of the shear flow can modify the relation between the period of the pattern and the amplitude of the magnetic field.

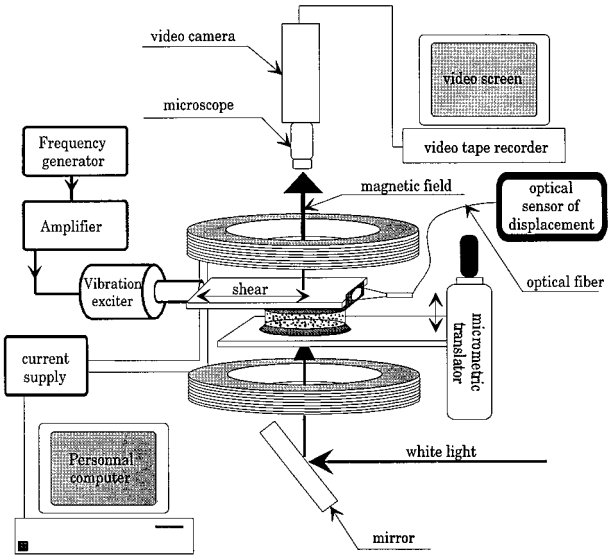

FIG. 1. Schematic view of the device used to study the shear-induced stripe pattern.

II. EXPERIMENTAL TECHNIQUE AND MATERIAL

In order to detect the changes of structure induced by a flow and a magnetic field, we have used the device shown in Fig. 1. The suspension is placed between two glass disks, the upper one is fixed on the arm of an electromagnetic vibrator and the lower one on a vertical micropositioner with submicrometer resolution on the displacement. On each disk, the side in contact with the suspension is coated with a transparent film of tin indium oxide. The presence of these two electrodes allows us to measure the capacity of the cell, with a Hewlett-Packard impedance analyzer. This is done by recording the change of capacity with the distance without bringing them into contact, which could destroy the adjustment of parallelism between the disks. This adjustment of parallelism is carried out by looking at the Fabry-Pérot fringes produced by the reflections of a laser beam between the two plates. The horizontality of the cell is also adjusted by using the reflections of the laser beam on the glass disks. The error on the parallelism is less than 3 μm across the whole surface and the error on the average thickness of the cell is less than 2 μm.

After the liquid has been introduced with a syringe, the lower plate is raised to a fixed distance from the upper one (less than 500 μm because the liquid is held by capillary forces). The horizontal displacement of the upper plate is measured with an optical detector, which detects the change of the light reflected by a small mirror mounted on the upper plate (cf. Fig. 1). The amplitude and frequency of the oscillatory motion are driven by a standard amplifier and a frequency generator. The field is set up with coils in a Helmholtz configuration and the images of the structure are recorded by an optical microscope and a video camera. The magnetic field is driven by a computer that also records the upper plate displacement.

The suspension we have used is made of polystyrene particles containing inclusions (63% by weight) of magnetite. These particles, designed by Rhône-Poulenc, are spherical but polydisperse with an average radius $a=0.24$ μm measured by dynamic light scattering. These particles behave as a superparamagnetic material: They do not show any magnetic hysteresis. The initial permeability μ_p of the particles was obtained from the magnetization of the sample measured with a vibrating magnetometer; we find $\mu_p=37$. The corresponding magnetic moment of a particle placed in the external magnetic field H_0 will be

$$m_p=4\pi\mu_0\beta a^3H_0, \quad \beta=(\mu_p-1)/(\mu_p+2).$$

We note that for high initial permeability, the factor β is close to unity and the magnetic moment becomes proportional to the volume of the particle. When we increase the field we observe a phase separation of the suspension into two phases: a concentrated one and a diluted one. In the absence of shear, the main quantity that will control this phase separation is the ratio of the magnetic dipolar energy to the thermal energy:

$$\lambda=\frac{m_p^2}{4\pi\mu_0(2a)^3kT}=\frac{\pi\mu_0a^3\beta^2H_0^2}{2kT}, \tag{1}$$

which gives, for $a=0.24$ μm, $\beta\approx1$ and room temperature $\lambda=6.7\times10^{-6}H_0^2$ (H_0 in A/m) or $\lambda=0.04B_0^2$ (B_0 in gauss). We see that even for fields as low as 5 G the magnetic force already dominates the thermal forces.

In the presence of a shear flow an additional parameter for structure formation is the Péclet number, which is the ratio between the hydrodynamic force $6\pi\eta\dot\gamma a^2$ induced by the shear rate $\dot\gamma$ on a particle and the thermodynamic force: kT/a. With the carrier fluid being water with a viscosity $\eta=10^{-3}$ Pa s we obtain

$$\mathrm{Pe}=\frac{6\pi\eta\dot\gamma a^3}{kT}=0.064\dot\gamma. \tag{2}$$

The Péclet number used in this work ranges from low (Pe=0.02) to high values (Pe=10), but it is worth noting that for all the results that will be presented in this paper, the magnetic forces dominate the shear forces; in other words, the Mason number Ma=Pe/λ is much lower than unity. This means that the flow only contributes to rearrange the structure but not to destroy it.

The shear rate $\dot\gamma$ in Eq. (2) is given by $\gamma\omega$, where $\gamma=x_0/h$ is the strain, h is the thickness of the cell, and x_0 is the amplitude of the oscillatory motion ($x=x_0\cos\omega t$). The frequency $f=\omega/2\pi$ of the oscillating shear flow was always lower than 10 Hz. In this range, we can consider that the shear flow is linear since the penetration length $\delta=\sqrt{\eta/\rho f}=330$ μm for $f=10$ Hz was larger than the thickness $h=100$ μm used for most of the experiments. The experiments done with a larger thickness were made at lower frequencies in order to fulfill this condition.

III. TRANSITION FROM CYLINDERS TO STRIPES

In the absence of a flow, the increase of the magnetic field involves a phase separation, whose characteristics have been reported elsewhere [8,9]. The structure formed during this phase separation consists of columnar aggregates that are located on a hexagonal network. Such a structure [cf. Fig. 2(a)] is only obtained if some special care is taken in order to

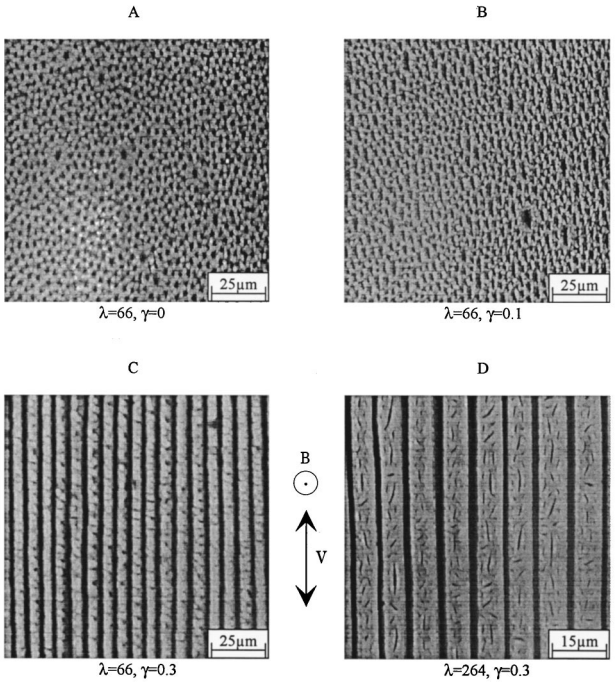

FIG. 2. Top view of the suspension recorded by a video camera. The field is perpendicular to the plane of the figure. (a) No flow, (b) oscillating shear flow with a strain $\gamma=0.1$, (c) same as (b) but with $\gamma=0.3$, and (d) same as (c) except the magnetic field, which has been multiplied by 2. Note the change of scale from (c) to (d).

avoid out-of-equilibrium configurations. This is achieved in the following way: The field is increased by steps of 0.1 Oe, the duration of one step is about 4 s, and then the field is switched off during a short period before it is increased again for the next step. In the interruption period, when magnetic forces between particles are absent, the particles can diffuse over a length comparable to their radius, which allows them to avoid being permanently trapped in a nonequilibrium configuration. The equilibrium structure formed in this way is hexagonal at least for not too high initial volume fractions. If we begin to shear this structure with a small strain ($\gamma<0.1$), the aggregates lose their cylindrical symmetry but remain well identified [cf. Fig. 2(b)]. Above a critical strain $\gamma_c=0.15$, there is a transition towards a striped structure with a well-defined period (approximately 7 μm), which is illustrated in Fig. 2(c). This critical strain characterizing the crossing from cylinders to stripes is independent of the cell thickness and the magnitude of the field. For volume fractions between 4% and 18%, there is also no change in this critical strain, at least within the uncertainty ($0.13<\gamma_c<0.17$), but for the lower volume fraction ($\phi=0.5\%$) we have found a different critical strain $\gamma_c=0.2$. At last, we have verified that this critical strain does not depend on the Péclet number. It then appears that the critical strain for the shear-induced transition between cylinders and stripes is quite independent of all the parameters.

A tentative interpretation of the critical strain may start from the comparison of the energy of the two different structures at zero strain. This calculation has been done in [11] and it is possible to calculate the change of energy due to the inclination of a cylindrical structure relatively to the field if we neglect the end effects due to the finite size of the sample

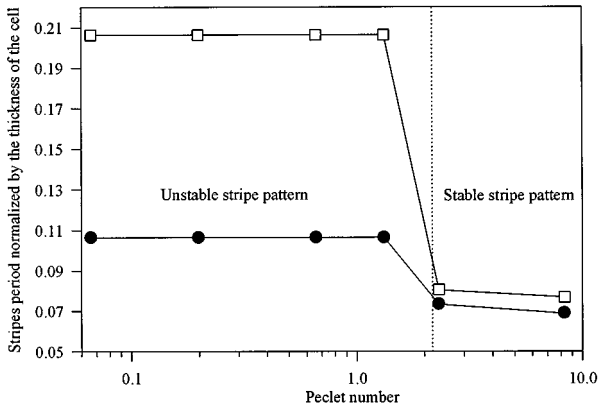

FIG. 3. Period of the layered structure versus the Péclet number for a given value of the magnetic field ($\lambda=55$). The upper curve is for a strain rate $\gamma=2$ and the lower curve for the critical strain rate $\gamma_c=0.15$.

[19]. The transition from cylinders to stripes is expected to occur for a strain γ_c such that the magnetic energy of the inclined cylinders reaches the energy of the stripe pattern. Note that this last energy should not change with the shear since the stripes are parallel to the velocity lines. This approach predicts a critical strain that is an order of magnitude lower than the experimental one. It probably indicates that the rearrangement from the cylinders to the stripes involves the passage by intermediate structures of higher energy, which makes it difficult to predict.

Let us now study the striped structure that is formed for strains larger than $\gamma_c=0.15$. The main feature characterizing this structure is its period d or, more exactly, a dimensionless period $d^*=d/h$, where h is the cell thickness. The study of this period with the different parameters ($\phi,\lambda,h,\mathrm{Pe}$) is the purpose of the next section.

IV. PERIOD OF THE STRIPES

In this section we are going to present the experimental results for the period of the structure and a model that will help us interpret the changes of the period relative to different parameters. This model is based on the assumption that the period can be obtained from the minimization of the free energy of the system even though this structure is formed by the application of a flow. Actually, as already pointed out, the magnetic forces dominate the hydrodynamic forces in all the situations we have studied, so we can expect that it is the magnetic energy that will drive the period of the structure. Before we introduce this model, let us present our main experimental findings.

A. Experimental results

In Fig. 3 we have plotted the dimensionless period d^* versus the Péclet number for two different strains $\gamma=0.15$ and 2, with a magnetic field corresponding to $\lambda=55$. In the low-Péclet-number region, a higher strain gives a larger period, but for a Péclet number above approximately 2, the period becomes independent of the strain. A still more interesting observation is that below this Péclet number of 2 the structures are not stable: If we stop the flow, the striped structure breaks down into a large number of small segments

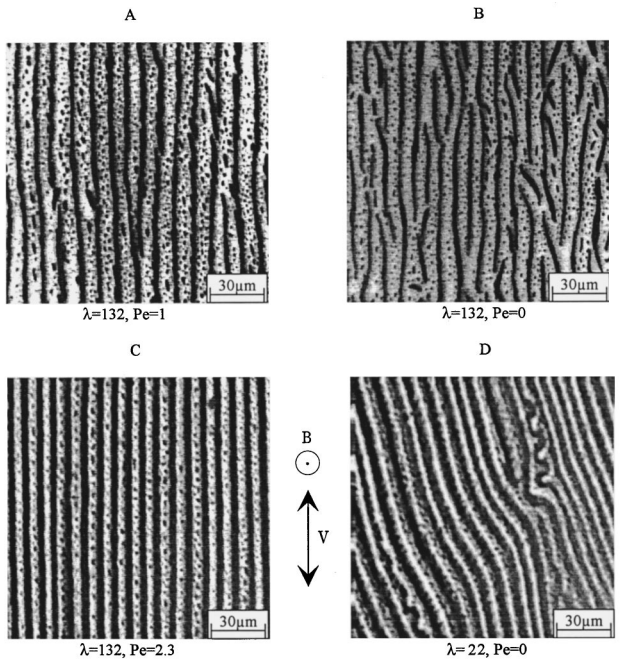

FIG. 4. Top view of the suspension recorded by a video camera. A layered structure (a) has been formed at low Péclet number; if we stop the flow, the layered structure breaks down (b). The layered structure (c) formed at high Péclet number (Pe=2.3) and high λ (λ=132) is stable even if we stop the flow. Then, decreasing the field, we obtain a bending instability (d).

that are disoriented with respect to the initial structure; this is illustrated in the upper part of Fig. 4. On the contrary, if we stop the flow after the structures have been formed at a high Péclet number and high λ, they remain stable if we keep the field constant. For instance, the pattern shown in Fig. 4(c) will remain identical if we stop the flow, but if we decrease the field, then the stripes begin to bend in order to decrease the distance between the layers and the pattern corresponds to the equilibrium values at lower field strength. This behavior is illustrated in Fig. 4(d), which is similar to the one observed in other smectic systems [2]. These two features [the stability of the stripes when the flow is stopped (keeping the same field) and the bending of the stripes if we decrease the field] seem to indicate that the structure formed for Pe>2 is an equilibrium structure. Actually, strictly speaking, it is a metastable structure since the stable structure in the absence of flow is a triangular network of cylinders but the difference in the energy between the two structures is small [11]. In the presence of the flow, the choice of the period d/h of the stripe pattern will correspond to a minimum of the magnetic energy only if hydrodynamic diffusion is high enough to help the particles find their optimum structure. Actually, these are likely fragments of chains, rather than individual particles, which are moving since, as previously stated, the hydrodynamic shear force on a pair of particles is always smaller than the magnetic force. Nevertheless, the hydrodynamic force dominates at the scale of aggregates since it increases linearly with the size of the object placed in the shear.

In the regime where the structure is stable after turning off the flow, we have measured the normalized period of the striped structure versus the external magnetic field H_0 for

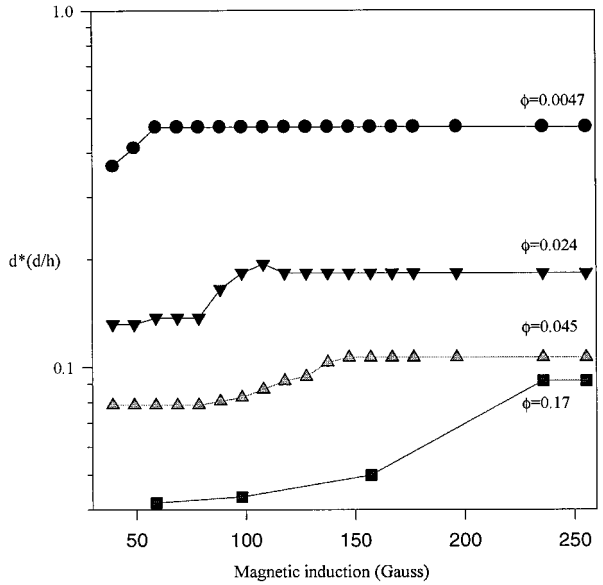

FIG. 5. Evolution of the period of the stable stripe pattern (Pe =2.3) with the field for different volume fractions.

different initial volume fractions. These results are summarized in Fig. 5. Two features are worth noting. First, we observe a decrease of the period when we increase the volume fraction. This is quite understandable since we know [11] that such a behavior is already true for the distance between aggregates in the absence of the flow. Nevertheless, this decrease is less pronounced at a high field than at a low field. The second, more surprising observation is that we found an increase of the period with the amplitude of the magnetic field. This can be noted by comparing Figs. 2(c) and 2(d): The period changes from 6.5 to 9 μm when the field is multiplied by a factor of 2 (pay attention to the change of scale). In ferrofluids, the opposite behavior is observed. This increase of the period takes place in a range of magnetic field that depends on the initial volume fraction (cf. Fig. 5). In order to understand these behaviors we have postulated a model based on a minimization of the magnetic energy, which is the object of the next subsection.

B. Model for the period of the striped structure

The schematic view of the striped structure is shown in Fig. 6 and we shall use the following notations for the magnetization: M_a is the magnetic moment of one stripe and V_a

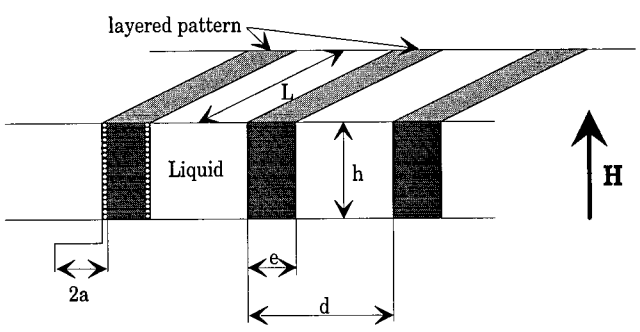

FIG. 6. Schematic view of the stripe structure with the notations used in this paper.

is its volume; $M_1 = M_a/V_a$ is the magnetization inside each stripe and $M = M_1\varphi$ is the average magnetization of the sample. The quantity $\varphi = e/d$ is the apparent volume fraction of the stripes, that is, the part of space that is occupied by the stripes. It must not be confused with the internal volume fraction inside the stripes $\phi_a = \phi/\varphi$, with ϕ the average volume fraction of the suspension. The magnetic energy of the system is obtained from the product of the total magnetic moment of the sample and the external field

$$\frac{U_m}{V} = -\frac{1}{2V} N_a \mathbf{M}_a \cdot \mathbf{H}_0 = -\frac{1}{2} \varphi \mathbf{M}_1 \cdot \mathbf{H}_0, \tag{3}$$

where N_a/V is the number of stripes per unit volume. M_1 can be calculated from the magnetic moment m_p of a particle inside the stripe. We have

$$M_1 = \frac{\phi_a}{\frac{4}{3}\pi a^3} m_p, \tag{4}$$

with

$$m_p = 4\pi\mu_0 \beta a^3 H_{\mathrm{loc}}, \tag{5}$$

where β is the same quantity as in Eq. (1). Here, instead of the external field that has been used to define λ we must consider the local field H_{loc} on the particle. This local field is the external field H_0 minus the demagnetizing field, which comes from the magnetization M_1, plus the Lorentz field:

$$H_{\mathrm{loc}} = H_0 - \frac{DM_1}{\mu_0} + \frac{M_1}{3\mu_0}. \tag{6}$$

Here D is the demagnetizing factor related to the stripe pattern. It is given by [2]

$$D(\varphi, d^*) = \left\{ \varphi + \frac{d^*}{\pi^3 \varphi} \sum_{n=1}^{\infty} \frac{\sin^2(\pi n \varphi)}{n^3} \times \left[1 - \exp\left(-\frac{2\pi n}{d^*} \right) \right] \right\}. \tag{7}$$

In Eq. (6) the quantity $H = H_0 - DM_1/\mu_0$ is the average field on a scale larger than the typical size of the structure. The local field is obtained with the trick of the Lorentz cavity. If we assume that the width of a stripe is much larger than the diameter of the particle, we can take a Lorentz sphere inside the stripe with a Lorentz field $H_{\mathrm{loc}} = M_1/3\mu_0$. From Eqs. (3)–(7) we obtain for the magnetization M_1 of a stripe:

$$M_1 = \mu_0 \chi_a^0 H_0 \quad \text{with} \quad \chi_a^0 = \frac{3\beta\phi_a}{1 + 3\beta\phi_a (D - \frac{1}{3})}. \tag{8}$$

Inserting this expression for M_1 into Eq. (3) gives the value of the magnetic energy per unit volume

$$\frac{U_m}{V} = -\frac{1}{2} \varphi \mu_0 H_0^2 \chi_a^0. \tag{9}$$

We have to introduce also the surface tension of the stripes σ. The corresponding energy per unit volume is

$$\frac{U_\sigma}{V} = \frac{2\sigma}{d}. \tag{10}$$

In this model we have two unknowns: φ and d. Now, if we assume that the fraction φ of the space occupied by the stripes does not depend on the period, the period is obtained by minimization of the total energy, for a given value of φ, relative to the period:

$$\left. \frac{\partial[(U_m/V) + (U_\sigma/V)]}{\partial d} \right|_\varphi = 0. \tag{11}$$

From Eqs. (3), (9), and (10) we obtain

$$\varphi \left. \frac{M_1^2 \partial D}{2\mu_0 \partial d} \right|_\varphi = \frac{2\sigma}{d^2}. \tag{12}$$

Equation (12) gives the period of the structure if we suppose that φ or equivalently the internal volume fraction ϕ_a (since $\varphi = \phi/\phi_a$) of the stripe pattern is known. In practice the dense phase is compressible and its volume fracion ϕ_a is unknown, except at high values of λ, where the increase of magnetic pressure should give a volume fraction close to the maximum packing fraction of the system. In the general case, we need an additional equation to obtain this internal volume fraction. It is based on a balance between the osmotic pressure P_{os}, which should destroy the stripes in the absence of the field, and the magnetic pressure p_m, which gives the attractive forces necessary to obtain this phase separation. The magnetic pressure is simply given by

$$p_m = -\left. \frac{\partial(U_m/V)}{\partial \varphi} \right|_d \tag{13}$$

or, from Eqs. (8) and (9) and taking into account that $\phi_a = \phi/\varphi$,

$$p_m = -\frac{M_1^2}{2\mu_0} \left(\frac{1}{3} - D + \varphi \left. \frac{\partial D}{\partial \varphi} \right|_d \right). \tag{14}$$

For the osmotic pressure we can use either the Carnahan-Starling expression (where $v = \frac{4}{3}\pi a^3$ is the particle volume)

$$p_{\mathrm{os}} = \frac{kT\phi_a(1 + \phi_a + \phi_a^2 - \phi_a^3)}{v(1 - \phi_a)^3} \tag{15}$$

or some *ad hoc* expressions that show better agreement with the pressure calculated by the numerical simulation for the internal volume fraction higher than 40% such as [20]

$$p_{\mathrm{os}} = \frac{kT 1.85 \phi_a}{v(0.64 - \phi_a)}. \tag{16}$$

In the following we shall use this expression where the value of 0.64 for the maximum volume fraction corresponds to an isotropic disordered medium. We could as well take the value of 0.69, which corresponds to the body-centered-tetragonal equilibrium structure of a monodisperse suspension in the limit of high λ, although this structure will not form with the rather polydisperse suspension we are using. In any event, we have found by using both 0.64 and 0.69 in

Eq. (16) that the dimensionless period was not very sensitive to this change of maximum volume fraction.

The internal volume fraction is obtained by balancing the osmotic and magnetic pressures

$$p_{\mathrm{os}}+p_m=0. \tag{17}$$

Equations (12) and (17) have to be solved simultaneously in order to obtain the equilibrium period and the internal volume fraction.

The surface energy σ is unknown; it is, by definition, related to the difference in energy between a particle located in the bulk of the stripe and on the edge. If we consider the magnetic particles to be hard spheres, the only interparticle force comes from the magnetic field. It is the difference between the local field inside the stripe and on the edge that will give the surface energy. It can be shown (cf. the Appendix) that this surface energy is proportional to the square of the magnetization and to the radius of the particles:

$$\sigma=C\,\frac{aM_1^2}{\mu_0}, \tag{18}$$

where C is a constant that takes the value $\frac{1}{3}$ if we use a mean-field approach. Using Eq. (18) and the definition of λ given by Eq. (1), Eqs. (12) and (17) become

$$\varphi\left.\frac{\partial D}{\partial d^*}\right|_{\varphi}=\frac{4Ca}{(d^*)^2h} \tag{19}$$

and

$$-12\lambda\left(\frac{\phi}{\varphi-\beta\phi(1-3D)}\right)^2\left(\frac{1}{3}-D+\varphi\left.\frac{\partial D}{\partial\varphi}\right|_{d^*}\right)+\frac{1.85\phi}{(0.64\varphi-\phi)}=0. \tag{20}$$

Equations (19) and (20) will allow us to calculate the equilibrium period d^* and the apparent volume fraction φ for a given value of the parameter λ (or, equivalently, H_0) and of the initial volume fraction ϕ. Note that in the derivation of Eq. (19) we have neglected the derivative of M_1^2, which is small relative to the term on the right-hand side of Eq. (19).

C. Comparison between theory and experiments

Before we test this model relative to the experimental results of Fig. 5, let us look at the dependence of the period on the thickness h of the cell. With our device, we can easily change the cell thickness, keeping unchanged the strain and the Péclet number by varying the amplitude x_0 and the frequency f of the oscillatory motion of the upper plate. We have plotted in Fig. 7 the evolution of the logarithm of the period d versus the logarithm of the cell thickness h for $\lambda=242$, Pe$=2.3$, $\phi=4.5\%$, and $\gamma=0.45$. The best fit with a straight line gives a slope of 0.56 and a fit with a slope of 0.50 is still compatible with the error bars. Actually, we can predict this behavior, $d\propto h^{0.5}$, if the normalized period $d^*=d/h$ remains small compared to unity (which is the case in all our experiments). Then we can neglect the exponential term in Eq. (7) and we get from Eq. (19)

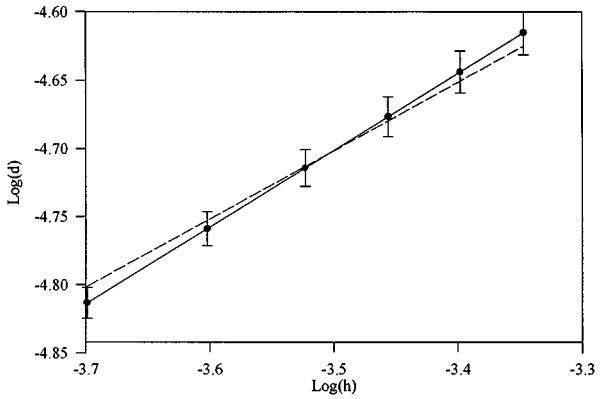

FIG. 7. Log_{10} of the period of the layered pattern versus the $\log_{10}$ of the cell thickness. ——, linear fit with slope 0.56; ----, linear fit with slope 0.50. Dots are experimental points.

$$d^2=\frac{4\pi^3Ca}{\sum_{n=1}^{\infty}\frac{\sin^2(\pi n\varphi)}{n^3}}\,h. \tag{21}$$

The prefactor of h contains the apparent volume fraction φ, which could be indirectly a function of h, because in the balance of magnetic and osmotic pressure, p_m depends on the demagnetization factor D. Nevertheless, for high values of λ, the magnetic pressure is high and the internal volume fraction ϕ_a inside the aggregates should be near its maximum. In these conditions we do not expect any significant change of φ with the cell thickness and the prefactor in Eq. (21) should remain constant, justifying the prediction $d\propto h^{0.5}$. This is fairly well verified experimentally.

The intersection with the origin, taking the value $\phi_a=0.64$, allows us to obtain the constant C appearing in the expression of the surface tension. We obtain $C=0.005$, which is very low compared to the value $\frac{1}{3}$ expected from the mean-field evaluation. We shall return to this point later. Taking this value of C, we can solve Eqs. (19) and (20) and predict the change of the period with the initial volume fraction. The result is shown in Fig. 8 (solid line) for a high value of λ ($\lambda=308$) together with the experimental points. The agreement is not perfect, especially for the lower volume fraction where the predicted period is two times the experimental one. Nevertheless, this model succeeds quite well in predicting a plateau for volume fractions higher than 4% and a strong increase at the lower volume fractions. It also predicts an increase of the period with the field, but the range of λ over which this increase should occur is two orders of magnitude lower than the experimental one, as we can see in Fig. 9 (solid line) for the volume fraction $\phi=4.5\%$.

Before we discuss this strong disagreement, let us determine the physical mechanism that produces an increase of the period with the field. If the internal volume fraction of the stripes is constant, then, as both the magnetic energy and the surface tension scale as M_1^2, we do not expect a change of period with the field, as can be seen from Eq. (19), which does not contain λ. If now we take into account that an increase of λ will increase the magnetic pressure and there-

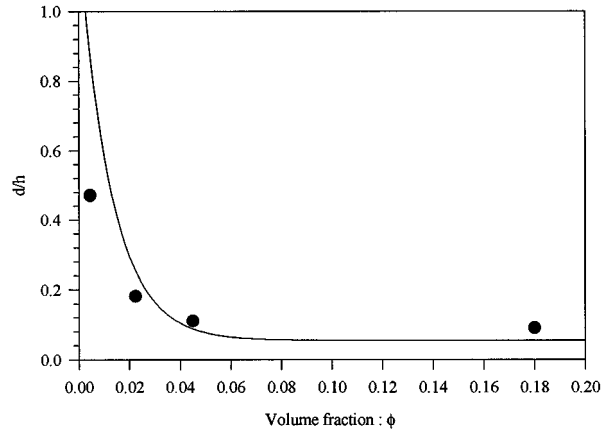

FIG. 8. Stripe period versus the initial volume fraction for $\lambda=264$. ——, theoretical predictions [Eqs. (19) and (20) with $C=0.005$]. Dots are experimental results.

fore ϕ_a, then the apparent volume fraction $\varphi=\phi/\phi_a$ will decrease along with the demagnetization factor D and the energy. This more favorable magnetic energy obtained by the increase of volume fraction inside the stripes allows us to find a new minimum of the energy for a larger period.

V. DISCUSSION

From this comparison between the experimental results and our model, we can conclude that the increase of the stripes period with the field, its decrease with the apparent volume fraction, and its behavior with the cell thickness are, quantitatively and qualitatively, described by a theory based on thermodynamic equilibrium in the absence of a flow. Nevertheless, two points remain unexplained. First, the surface energy determined experimentally from the dependence of the period on the cell thickness is much smaller than the value expected on the basis of a mean-field theory. Second, the range of magnetic energy that gives rise to the increase of the period is two orders of magnitude greater than the one predicted by the model (compare in Fig. 9 the dotted line to the filled circles). Concerning the low value of the surface energy, a possible explanation could be that the choice of a Lorentz sphere inside the stripe to calculate the local field is not appropriate for the particles on the edge of the stripe: The local order is anisotropic, the thickness of the stripes is only a few particles in diameter, and the dipolar interactions with the closest particles of the neighbor stripe can also modify this surface energy.

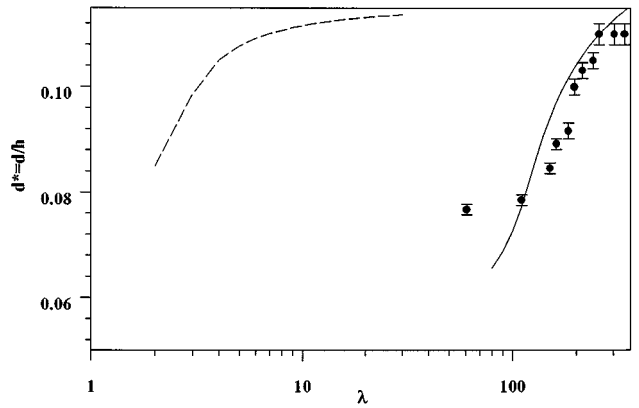

FIG. 9. Increase of stripe period with the magnetic field (expressed through λ) for the initial volume fraction ($\phi=4.5\%$). Dots are experimental results. ----, theoretical prediction without flow (Pe=0); ——, theoretical prediction with Pe=2.3.

Concerning the second point, we have to take into account the fact that the suspensions are not monodisperse. The standard deviation is about 10% and, even if a small fraction of particles has a diameter two times lower than the average diameter, the osmotic pressure that scales as the inverse of the cube of the radius could be much larger. Nevertheless, we should assume that the effect of the polydispersity is equivalent to lowering the average diameter by a factor of 3, which is clearly unacceptable. A more convincing explanation is obtained by considering the increase of the pressure normal to the plane of the stripes, which is due to the shear flow. This pressure comes from the shear force between two particles that scales as $6\pi\eta\dot{\gamma}a^2$; since the total pressure is normalized by kT/v, we shall have an extra term in the balance of pressure [Eq. (20)], which will be a function of the Péclet number [Eq. (2)] and will act in the same direction as the osmotic pressure. This pressure will increase with the internal volume fraction of the stripes and, as for all the components of the stress tensor, will diverge for the maximum packing fraction allowing a flow. We can choose the expression for the normal pressure given by Brady and coworkers [21,22], where the normal stress differences N_i $(i=1,2)$ are shown to diverge as $N_i/\eta\dot{\gamma}=(1-\phi_a/\phi_m)^{-2}P_e$ when $\overline{\mathrm{Pe}}\ll 1$. This quantity $\overline{\mathrm{Pe}}\approx \mathrm{Pe}\, D_0/D_0^s(\phi)$ is built from the diffusion coefficient at the actual volume fraction $D_0^s(\phi)$ rather than the diffusion coefficient of an isolated particle D_0. As $D_0^s\approx(1-\phi/\phi_m)$ for $\phi\to\phi_m$ this model predicts normal stresses and thus a pressure normal to the plane of the stripes, which scales as

$$p_h^*=(1-\phi_a/\phi_m)^{-3}\mathrm{Pe}^2. \tag{22}$$

For $\mathrm{Pe}\gg 1$ the scaling is different with a power -2 instead of -3. We have then added the term $(1-\phi_a/\phi_m)^{-2}\mathrm{Pe}^2$ to the left-hand side of Eq. (20). The result of the prediction is shown by the solid line in Fig. 9. The agreement with the experiment is much more satisfying. This improvement emphasizes the importance of the normal stress differences at least for low to intermediate values of λ. This finding is interesting since it gives a way to correlate the normal stress differences to the expansion of the width of the stripes. In particular, it is worth noting that, once the layered pattern has been formed in the presence of a flow, we can turn off the magnetic field and measure the hydrodynamic diffusive flux in the direction of the vorticity by recording the disappearance of the striped pattern. The relation between normal stresses and shear-induced diffusion is of interest in many fields related to the dynamics of suspensions [23] and this system offers several possibilities to study this relation.

VI. CONCLUSION

In this study of field-induced phase separation in the presence of a shear flow we have shown that a well-defined layered structure appears above a critical strain rate of 0.15.

This critical strain rate is independent of most of the parameters, but it increases slightly for the smaller volume fraction. If the layered pattern is formed at a low Péclet number, it breaks when the flow is stopped. This is not the case if the pattern is formed at a Péclet number higher than unity. In the latter case, the pattern is stable in the absence of a flow and if we decrease the magnetic field we observe a bending instability that is coherent with the fact that the period of the pattern decreases when the magnetic field decreases. These observations indicate that in order to attain an equilibrium structure we need a strong enough shear, able to overcome some potential barrier. For these equilibrium structures obtained at high values of λ we can predict the evolution of the period with the cell thickness or with the initial volume fraction, without taking into account explicitly the effect of the flow. The agreement of the model with the experiments is even quantitative except for the prediction of the increase of the period with λ, at intermediate values of λ. In this range of λ where the maximum volume fraction inside the stripes is not reached, the effect of the shear flow is to enhance the hydrodynamic diffusion and hence the apparent volume fraction of the stripes. This effect needs to be investigated in more detail in future work in addition to the value of the critical strain rate γ_c for other magnetic suspensions.

ACKNOWLEDGMENTS

We wish to thank L. Lobry and P. Lanson for their measurement of the sizes of the particles and Dr. J. Richard from Rhône-Poulenc, who provides us with the samples of magnetic fluids and J. Brady for his helpful comments. A.C. was supported by a grant from the French foreign office during his stay at the University of Nice.

APPENDIX: DERIVATION OF EQ. (18) FOR THE SURFACE TENSION

The particles that are at the interface between the dense phase and the suspending fluid experience a local field that is different from the local field inside the stripe. If we assume that the magnetization is constant everywhere in the stripe and zero in the suspending fluid, then the Lorentz field for a particle on the boundary comes from the integral of $\mathbf{M}_1 \cdot \mathbf{n}$ on a half sphere with $\mathbf{n}$ the normal to the Lorentz sphere. This will give

$$H_{\mathrm{loc}} = H_0 - D\,\frac{M_1}{\mu_0} + \frac{1}{2}\,\frac{M_1}{3\mu_0}$$

instead of Eq. (6). Taking into account that the fraction of particles on the surface is $4a/e$ gives a modified magnetization of the stripe with $D - \frac{1}{3} + \frac{2}{3}a/e$ instead of $D - \frac{1}{3}$ in the denominator of χ_0^a [Eq. (8)]. Then if a/e is small compared to unity we can develop the magnetic energy as

$$\frac{U_m}{V} = -\frac{1}{2}\,\varphi\mu_0 H_0^2 \chi_a^0 + \frac{\varphi M_1^2}{3\mu_0}\,\frac{a}{e};$$

The second term is the surface energy appearing in Eq. (10). If we identify it with Eq. (10), taking $\varphi = e/d$, we obtain

$$\sigma = \frac{a}{3\mu_0}\,M_1^2.$$

[1] M. Seul and D. Andelman, Science **267**, 476 (1995).
[2] C. Flament, J. C. Bacri, A. Cèbers, F. Elias, and R. Perzynski, Europhys. Lett. **34**, 225 (1996).
[3] M. Seul and R. Wolfe, Phys. Rev. A **46**, 7519 (1992).
[4] A. C. Newell, T. Passot, N. Ercolani, and R. Indik, J. Phys. II **5**, 1863 (1995).
[5] A. Cebers, Magn. Gidrodin. **3**, 49 (1990); [Magnetohydrodynamics **96**, 309 (1990)].
[6] Yu. A. Buyevich and A. Yu. Zubarev, J. Phys. II **3**, 1633 (1993).
[7] H. M. McConell, Proc. Natl. Acad. Sci. USA **86**, 3452 (1989).
[8] E. Lemaire, G. Bossis, and Y. Grasselli, J. Phys. II **2**, 359 (1992).
[9] J. Liu *et al.*, Phys. Rev. Lett. **74**, 2828 (1995).
[10] E. Lemaire (private communication).
[11] A. Cebers, Prog. Colloid Polym. Sci. **100**, 101 (1996).
[12] G. Bossis, Y. Grasselli, E. Lemaire, L. Petit, and J. Persello, Europhys. Lett. **25**, 335 (1994).
[13] J. R. Melrose, Phys. Rev. A **44**, R4789 (1991).
[14] J. M. Sun and R. Tao, Phys. Rev. E **53**, 3732 (1996).
[15] J. H. E. Promislow and A. P. Gast, Langmuir **12**, 4095 (1996).
[16] G. Bossis and A. Cebers, Magn. Gidrodin. (to be published).
[17] Th. C. Halsey and W. Toor, Phys. Rev. Lett. **65**, 2820 (1990).
[18] H. J. H. Clercx and G. Bossis, J. Chem. Phys. **98**, 8284 (1993).
[19] G. Bossis, E. Lemaire, O. Volkova, and H. J. H. Clercx, J. Rheol. **47**, 687 (1997).
[20] W. B. Russel, D. A. Saville and W. R. Schowalter, *Colloidal Dispersions* (Cambridge University Press, Cambridge, 1989).
[21] J. F. Brady and M. Vicic, J. Rheol. **39**, 545 (1995).
[22] J. F. Brady and J. F. Morris, J. Fluid Mech. (to be published).
[23] A. W. Chow, S. W. Winton, J. H. Iwamiya, and T. S. Stephens, Phys. Fluids **6**, 2561 (1994).